COMPDYN 2011
III ECCOMAS Thematic Conference on
Computational Methods in Structural Dynamics and Earthquake Engineering
M. Papadrakakis, M. Fragiadakis, V. Plevris (eds.)
Corfu, Greece, 26–28 May 2011

NUMERICAL AND EXPERIMENTAL ASSESSMENT OF VARIOUS NON-CLASSICAL METHODS FOR PARAMETRIC IDENTIFICATION OF NONLINEAR VISCOUS DAMPERS

Jennifer Avakian[1], Giuseppe Carlo Marano[1], Giorgio Monti[2] , Giuseppe Quaranta[2] and F. Trentadue[1]

[1] Dept. of Environmental Engineering and Sustainable Development, Technical University of Bari
viale del Turismo 10, 74100, Taranto, Italy {jeneva,g.marano}@poliba.it

[2] Dept. of Structural Engineering and Geotechnics, Sapienza University of Rome
via A. Gramsci 53, 00197, Roma, Italy {giorgio.monti,giuseppe.quaranta}@uniroma1.it

Keywords: Differential Evolution, Genetic Algorithm, Parametric Identification, Particle Swarm Optimization, Viscous Damper.

Abstract. *Passive strategies based on the introduction of energy dissipating devices into the structures have received considerable attention in recent years. Within this framework, as reliable and cheap energy-dissipation devices, viscous fluid dampers have been largely used in seismic protection of industrial machines, technical equipments, buildings and bridges. Since the versatility of this passive protection system satisfactorily meets a wide range of requirements, a reliable identification of their nonlinear mechanical behavior is of outstanding importance. This paper focuses on the parametric identification of fractional derivative based models for nonlinear viscous dampers by means of non-classical methods, which are unconventional algorithms whose inner work is based on socially, physically and/or biologically inspired paradigms. Non-classical strategies are potentially powerful tools for solving complex identification problems because of their start-point independence, noise robustness and the capability in looking for the best solution in a global way. In contrast, it is important to highlight that they typically possess weak forms of convergence. For better assessing the correctness of some non-classical methods in parametric identification of viscous dampers, we perform a large comparative analysis which involve the following soft computing based techniques: a multi-species genetic algorithm, six standard differential evolution algorithms and four swarm intelligence based algorithms (including a chaotic particle swarm optimization algorithm). A numerical study is initially conducted in order to investigate the general reliability of these methods. Moreover, the paper also provides some results about the parametric identification of nonlinear viscous dampers by using experimental data. A critical review of the obtained evidences is given in order to provide useful guidelines for similar engineering applications.*

1 INTRODUCTION

Existing strategies for enhancing structural performances and safety against natural and manmade hazards can be grouped into three broad areas: base isolation, passive energy dissipation and active control. Passive energy dissipation systems can be realized by using a very wide range of materials and devices for enhancing damping, stiffness and strength. They can be used both for seismic hazard mitigation and for rehabilitation of aging or deficient structures. These devices generally operate on principles such as frictional sliding, yielding of metals, phase transformation in metals, deformation of viscoelastic solids or fluids and fluid orificing [1]. In this paper, the attention is focused on viscous damper devices whose most interesting features are: (*i*) low maintenance costs; (*ii*) usability for several severe earthquakes without damage; and (*iii*) forces exerted by the damper devices do not increase the stress in the structural system, being out of phase with the elastic forces. A viscous fluid damper typically consists of a piston within a damper housing filled with a compound of silicone or similar type of oil. Through a number of small orifices, the fluid pass from one side of the piston to the other: therefore, this device is able to dissipate energy through the movement of a piston in a highly viscous fluid based on the concept of fluid orificing [1]. Nowadays, a large number of civil engineering structures (buildings as well as bridges) is equipped with viscous fluid dampers in order to control seismic or wind induced motions and thermal expansions.

Since the applications of viscous dampers is growing very fast, their characteristics must be carefully investigated in order to provide a reliable support for designing an efficient protection strategy. Because of their inherent nonlinear behavior, condition assessment techniques require appropriate identification techniques. For instance, several identification approaches, both parametric and nonparametric, are compared in [2] by using real data carried out from full-scale nonlinear viscous dampers commonly used with large flexible bridges. About the parametric techniques, in [2] are explored the capability of the Adaptive Random Search: to this end, the authors solved an optimization problem in which the numerical values of the unknown model parameters were estimated by minimizing an objective function based on the normalized mean square error between the measured and identified damper responses. Since its weak form of convergence, the Adaptive Random Search belongs to the class of non-classical identification techniques [3], which are unconventional numerical identification methods mostly based on socially, physically and/or biologically inspired paradigms (i.e., ant colony based algorithms, artificial neural networks, differential evolution algorithms, genetic algorithms, genetic programming, particle swarm optimization algorithms, etc.).

This paper provides a comprehensive investigation about the parametric identification of viscous dampers via non-classical methods. To this end, we perform a large comparative analysis in which the following soft computing based techniques are examined: a special multi-species genetic algorithm, six standard differential evolution algorithms and four swarm intelligence based algorithms (including a chaotic particle swarm optimization algorithm). A numerical study is initially conducted in order to investigate the general reliability of these methods. Moreover, the paper also provides some results about the parametric identification of a full-scale nonlinear viscous damper by using experimental data. A critical review of the obtained evidences is given in order to provide useful guidelines for similar engineering applications.

2 PARAMETRIC IDENTIFICATION OF VISCOUS DAMPERS

The application of non-classical methods for the parametric identification of viscous dampers requires (i) the definition of an appropriate single-degree-of-freedom mechanical model and (ii) the formalization of the objective (or cost) function to be minimized.

2.1 Dynamic models

The damper effect is an output resistive force, therefore it acts in the opposite direction to that of the relative velocity between the ends of the damper device itself. The typical damping force ψ_d is:

$$\psi_d = C_\alpha \mathrm{sgn}\left[\dot{y}\right]\left|\dot{y}\right|^\alpha \tag{1}$$

where y is the displacement time-history (the time variable t is omitted for the sake of conciseness, the upper dots indicate the time-derivative). Moreover, sgn[·] is the signum function, C_α is the damping coefficient and α is the damping law exponent. The value of α for seismic applications ranges between 0.10 and 0.50 (in this way the force rises very fast for small velocity values and becomes almost constant for large velocity values). Regarding the elastic force ψ_e, both linear and parabolic models were investigated in [4]:

$$\psi_e = K_1 y \tag{2}$$

$$\psi_e = K_2 y^2 + K_1 y + K_0 \tag{3}$$

in which K_1 is the elastic stiffness, K_2 and K_0 are two constants. In [4] is stated that the parabolic function reproduces the shape of the test cycles more precisely, but the linear one may be preferred because it is more simple and yields a comparable energy balance. By combining Eq. (1) and Eq. (2), the equation of motion of a fractional viscous damper system subjected to a time-varying force p is [4]:

$$M\ddot{y} + C_\alpha \mathrm{sgn}\left[\dot{y}\right]\left|\dot{y}\right|^\alpha + K_1 y = p \tag{4}$$

where M is the effective mass. If the parabolic model given by Eq. (3) is taken into account, then the equation of motion becomes [4]:

$$M\ddot{y} + C_\alpha \mathrm{sgn}\left[\dot{y}\right]\left|\dot{y}\right|^\alpha + \left(K_2 y^2 + K_1 y + K_0\right) = p \tag{5}$$

In [5] are considered a fraction viscous model and a linear one as follows:

$$M\ddot{y} + C_1\dot{y} + C_\alpha \mathrm{sgn}\left[\dot{y}\right]\left|\dot{y}\right|^\alpha + K_1 y = p \tag{6}$$

where C_1 is the internal damping coefficient.

The system response can be determined as solution of the considered equation of the motion by using standard numerical time-marching techniques if the initial conditions and the values of the system parameters are known.

2.2 Parametric identification

The model parameters $\mathbf{x}$ of the viscous damper are identified by solving the following single-objective optimization problem :

$$\begin{aligned} &\min_{\mathbf{x}} \left\{ f\left(\mathbf{x}\right)\right\} \\ &\text{s.t. } \mathbf{x}^l \le \mathbf{x} \le \mathbf{x}^u \end{aligned} \tag{7}$$

in which $\mathbf{x}^l$ and $\mathbf{x}^u$ are the lower and upper bounds of the system parameters, respectively.

The objective or cost function $f(\mathbf{x})$ is:

$$f\left(\mathbf{x}\right) = \frac{100}{S\sigma_y^2}\sum_{s=1}^{S}\left(y_s - y_s^*\left(\mathbf{x}\right)\right) \tag{8}$$

where y_s is the measured displacement, y_s^* is the computed displacement, S is the number of data points (s is a generic sample index) and σ_s^2. The cost function in Eq. (8) coincides with that in [2] as the weight for the velocity-based addend is equal to zero. In fact, although the information regarding the velocity response may help the parametric identification, it introduces some additional complications. First, the velocity response is not typically measured, so that it needs to be calculated from the displacement response. Second, the weights of a mixed displacement-velocity cost function should be tuned for better matching the experimental data, and thus it requires preliminary user-supervised runs. On the other hand, the objective function in Eq. (8) can be directly used with experimental data without preliminary runs.

The Adaptive Random Search was used in [2] to solve a single-objective optimization problem as in Eq. (7) in order to identify the system parameter **x**. In this paper, we perform comparative analyses involving differential evolution, particle swarm optimization and genetic algorithm.

3 IDENTIFICATION VIA DIFFERENTIAL EVOLUTION

Differential evolution algorithm (DEA) is a relatively recent stochastic, population-based global optimization method whose positive features are attracting the interest of several researches in the field of the applied sciences. Different from traditional evolutionary algorithms, this optimizer is completely self-organizing and requires few lines of code in most of the existing programming languages. Moreover, its functionality requires a small set of embedded control parameters, which makes it easy to use for non-experts.

3.1 Mutation operators

The standard version of the DEA [1] uses the differences between randomly selected individuals as the source of random variations for a third individual referred to as the target vector. Trial solutions are generated by adding weighted difference vectors to the target vector. This process is dubbed mutation operator: its main goal is to enable diversity in the current population as well as "to move" the individuals in such a way a better result is expected. By computing the differences between two individuals randomly chosen from the population, the algorithm estimates the gradient in that zone rather than in a single point of the search space. Let us consider ${}^k\mathbf{x}_i=\{{}^kx_{i1},\ldots,{}^kx_{ij},\ldots,{}^kx_{in}\}$ the ith individual (with $i=1,\ldots,N$) at iteration k. The initial population ${}^0\mathbf{x}_i$ for $i=1,\ldots,N$ is defined by generating randomly the collection of N solutions within the specified search space. During the iteration $k+1$, for each individual ${}^k\mathbf{x}_i$ a mutation vector ${}^{(k+1)}\mathbf{z}_i$ is computed by using one of the following alternatives:

$$ {}^{(k+1)}\mathbf{z}_i = {}^k\mathbf{x}_{r1} + F^1\left({}^k\mathbf{x}_{r2} - {}^k\mathbf{x}_{r3}\right) \tag{9} $$

$$ {}^{(k+1)}\mathbf{z}_i = {}^k\mathbf{x}_{best} + F^1\left({}^k\mathbf{x}_{r1} - {}^k\mathbf{x}_{r2}\right) \tag{10} $$

$$ {}^{(k+1)}\mathbf{z}_i = {}^k\mathbf{x}_i + F^2\left({}^k\mathbf{x}_{best} - {}^k\mathbf{x}_i\right) + F^1\left({}^k\mathbf{x}_{r1} - {}^k\mathbf{x}_{r2}\right) \tag{11} $$

$$ {}^{(k+1)}\mathbf{z}_i = {}^k\mathbf{x}_{best} + F^2\left({}^k\mathbf{x}_{r1} - {}^k\mathbf{x}_{r2}\right) + F^1\left({}^k\mathbf{x}_{r3} - {}^k\mathbf{x}_{r4}\right) \tag{12} $$

$$ {}^{(k+1)}\mathbf{z}_i = {}^k\mathbf{x}_{r1} + F^2\left({}^k\mathbf{x}_{r2} - {}^k\mathbf{x}_{r3}\right) + F^1\left({}^k\mathbf{x}_{r4} - {}^k\mathbf{x}_{r5}\right) \tag{13} $$

where $r1$, $r2$, $r3$ and $r4$ denote integers randomly selected within the set $\{1,\ldots,i\text{-}1,i\text{+}1,\ldots,N\}$ such that $r1\neq r2\neq r3\neq r4$. The individual ${}^k\mathbf{x}_{best}$ is the best performer in the population at iteration k. The coefficients F^1 and F^2 are the so-called mutation coefficients and they are real positive constants whose typical values are in the range [0.40,1.00], 0.50 in our numerical applications.

These parameters control the amplification level of the mutation (for this reason they are also dubbed "scale factors").

3.2 Crossover operator

The crossover follows the mutation phase. For each mutated vector ${}^{(k+1)}\mathbf{z}_i$ a trial vector ${}^{(k+1)}\mathbf{u}_i$ (offspring) is generated by using the following so-called binomial crossover:

$$ {}^{(k+1)}u_{ij} = \begin{cases} {}^{(k+1)}z_{ij} & \text{if } q \le p^c \text{ or } j = randint(1,n) \\ {}^{k}x_{ij} & \text{otherwise} \end{cases} \tag{14} $$

where q is a random number generated by using the uniform probability density function in the range [0,1]. The parameter p^c is the probability of crossover and it takes values between 0 and 1 (usually, 0.50). Moreover, *randint*(1,*n*) is an integer randomly selected within the set $\{1,\ldots,n\}$ and it is adopted to ensure that at least one parameter is taken into account for constructing the vector ${}^{(k+1)}\mathbf{u}_i$.

3.3 Selection operator

An opportune strategy is needed to ensure the feasibility of the obtained solutions in Eq. (14), that means the fulfillment of both lower and upper bounds of the search space: in this paper, if a vector out-of-range is obtained, then its projection on the prescribed interval is considered (so-called projection scheme). Subsequently, the selection operator is performed by means of a very simple one-to-one competition scheme between ${}^{(k+1)}\mathbf{u}_i$ and ${}^{(k+1)}\mathbf{x}_i$ as follows:

$$ {}^{(k+1)}\mathbf{x}_i = \begin{cases} {}^{(k+1)}\mathbf{u}_i & \text{if } f\left({}^{(k+1)}\mathbf{u}_i\right) < f\left({}^{(k+1)}\mathbf{x}_i\right) \\ {}^{k}\mathbf{x}_i & \text{otherwise} \end{cases} \tag{15} $$

Therefore the winner ${}^{(k+1)}\mathbf{x}_i$ in the selection stage is the best performer between the parent individual ${}^{k}\mathbf{x}_i$ and its trial one ${}^{(k+1)}\mathbf{u}_i$. The output of this operator is a new population for the next generation, unless a stopping criteria has not been fulfilled. In this study, we will stop the evolutionary search once a maximum number of iterations L is achieved.

3.4 An adaptive mutation operator

In [7] is presented a mutation operator in which only one control parameter is required and the mutation coefficients are adaptive. The mutation operator proposed in [7] deals with the following revised version of Eq. (11):

$$ {}^{(k+1)}\mathbf{z}_i = {}^{k}\mathbf{x}_i + {}^{k}F_{r3,i}\left({}^{k}\mathbf{x}_{r3} - {}^{k}\mathbf{x}_i\right) + {}^{k}F_{r1,r2}\left({}^{k}\mathbf{x}_{r1} - {}^{k}\mathbf{x}_{r2}\right) \text{ if } k \le \kappa L \tag{16} $$

and

$$ {}^{(k+1)}\mathbf{z}_i = {}^{k}\mathbf{x}_{r1} + {}^{k}F_{best,i}\left({}^{k}\mathbf{x}_{best} - {}^{k}\mathbf{x}_i\right) + {}^{k}F_{r1,r2}\left({}^{k}\mathbf{x}_{r1} - {}^{k}\mathbf{x}_{r2}\right) \text{ if } k > \kappa L \tag{17} $$

where κ is the only one control parameter. The adaptive mutation coefficients in Eq. (16) and in Eq. (17) are calculated as follows:

$$ {}^{k}F_{r3,i} = \max\left\{\left|\frac{f\left({}^{k}\mathbf{x}_{r3}\right) - f\left({}^{k}\mathbf{x}_i\right)}{{}^{k}f_{\max} - {}^{k}f_{\min}}\right|, 0.5\right\} \tag{18} $$

$$ {}^{k}F_{r1,r2} = \begin{cases} \max\left\{ \left| \dfrac{f\left({}^{k}\mathbf{x}_{r1}\right) - f\left({}^{k}\mathbf{x}_{r2}\right)}{{}^{k}f_{\max} - {}^{k}f_{\min}} \right|, 0.5 \right\} & \text{if } k \le \kappa L \\ \left| \dfrac{f\left({}^{k}\mathbf{x}_{r1}\right) - f\left({}^{k}\mathbf{x}_{r2}\right)}{{}^{k}f_{\max} - {}^{k}f_{\min}} \right| & \text{if } k > \kappa L \end{cases} \tag{19} $$

$$ {}^{k}F_{best,i} = \left| \frac{{}^{k}f_{\min} - f\left({}^{k}\mathbf{x}_{i}\right)}{{}^{k}f_{\max} - {}^{k}f_{\min}} \right| \tag{20} $$

in which:

$$ \begin{aligned} {}^{k}f_{\min} &= \min_{i=1,\ldots,N}\left\{ f\left({}^{k}\mathbf{x}_{i}\right)\right\} \\ {}^{k}f_{\max} &= \max_{i=1,\ldots,N}\left\{ f\left({}^{k}\mathbf{x}_{i}\right)\right\} \end{aligned} \tag{21} $$

Taking into account this operator, the mutation occurs in two distinct ways. The first one takes place when $k \le \kappa L$ and its goal is to help the exploration of the search space. In this effort, the weighted difference vectors in Eq. (16) only involves randomly selected individuals and the mutation coefficients are forced to be greater than 0.5, see Eq. (18) and the first equality in Eq. (19). Once $k > \kappa L$, the mutation scheme proposed in Eq. (19) is performed. In this case, the current best individual ${}^{k}\mathbf{x}_{best}$ is taken into account. Substantially, the goal of this alternative scheme is to keep track of the current best performer within the population. Moreover, an improved exploitation can be achieved by removing the lower bounds for the adopted mutation coefficients (therefore numerical values less than 0.50 are accepted at this time). However, there is not rigid separation between exploration and exploitation because the numerical values of the scale factors are dynamically adjusted during the evolutionary search (adaptive property): for instance, if the exploration of the search space is not concluded for $k \le \kappa L$ then the numerical values of the mutation remain sensibly large and the global recognition is not penalized. Our numerical analyses – on both mathematical and engineering problems – demonstrate that a good value for κ (the only parameter of the proposed mutation operator) should be selected within 0.40 and 0.60, κ=0.50 in this paper.

3.5 A free-parameter crossover operator

The binomial scheme in Eq. (14) was replaced in [7] with the following one:

$$ {}^{(k+1)}\mathbf{u}_i = {}^{(k+1)}\mathbf{q}_i \times {}^{k}\mathbf{x}_i - \left(\mathbf{1} - {}^{(k+1)}\mathbf{q}_i\right) \times {}^{(k+1)}\mathbf{z}_i \tag{22} $$

where ${}^{(k+1)}\mathbf{q}_i$ is a vector whose n components are random numbers generated by using the uniform probability density functions in the range [0,1]. Moreover, $\mathbf{1}=\{1_1,\ldots,1_j,\ldots,1_n\}$. The results of the binomial crossover in Eq. (14) are vertex points of the hypercube defined by ${}^{(k+1)}\mathbf{z}_i$ and ${}^{(k+1)}\mathbf{x}_i$. Similarly, these vertex points are possible solutions of the crossover operator presented in Eq. (22) when ${}^{(k+1)}q_{ij} \to 0$ or ${}^{(k+1)}q_{ij} \to 1$ for each $j=1,\ldots,n$. Additionally, this crossover operator allows the exploration of the inner space bounded by this hypercube. It is evident that the probability of reproduction is not required for performing the proposed crossover, and thus Eq. (22) is a free-parameter operator.

4 IDENTIFICATION VIA PARTICLE SWARM OPTIMZIATION

Based on the swarm intelligence theory, two different categories of optimizers can be formulated:

- Particle swarm optimization algorithms (PSOAs) in which is assumed that a Newtonian dynamic regulates the movement of the particles. Therefore, position and velocity can be determined simultaneously.
- Quantum-behaved particle swarm optimization algorithms (Q-PSOAs) in which the Newtonian hypothesis is rejected. In this case, the classical mechanic is replaced with the quantum mechanics in which the term "trajectory" is meaningless [8].

The first class of PSOAs is the object of investigation in this paper.

4.1 General model

The ith particle (with i=1,…,N) at iteration k has two attributes, that are its velocity ${}^{k}\mathbf{v}_i=\{{}^{k}\mathbf{v}_{i1},\ldots,{}^{k}\mathbf{v}_{ij},\ldots,{}^{k}\mathbf{v}_{in}\}$ and position ${}^{k}\mathbf{x}_i=\{{}^{k}\mathbf{x}_{i1},\ldots,{}^{k}\mathbf{x}_{ij},\ldots,{}^{k}\mathbf{x}_{in}\}$. To protect the cohesion of the swarm the velocity ${}^{k}\mathbf{v}_{ij}$ is forced to be (in absolute value) less than a maximum velocity $v_j^{\max}$ with $\mathbf{v}^{\max}=\{v_1^{\max},\ldots, v_j^{\max},\ldots,v_n^{\max}\}$. Typically, it is assumed $\mathbf{v}^{\max}=\gamma(\mathbf{x}^u - \mathbf{x}^l)/\tau$ (the time factor τ = 1 is introduced to assign a physical meaning to the formula) but there is not sufficient degree of uniformity about γ whose numerical value can vary in a large interval (usually its value is 0.50). The initial positions ${}^{0}\mathbf{x}_i$ for i=1,…,N are defined by generating randomly the collection of N solutions within the assigned search space. Moreover, ${}^{0}v_{ij}$ is randomly generated using an uniform distribution between $-v_j^{\max}$ and $+v_j^{\max}$. At iteration k+1 the velocity ${}^{(k+1)}\mathbf{v}_i$ and the position ${}^{(k+1)}\mathbf{x}_i$ are evaluated as follows [9]:

$$ {}^{(k+1)}\mathbf{v}_i = w\,{}^{k}\mathbf{v}_i + c_1\,{}^{(k+1)}\mathbf{r}_{i1}\times\left({}^{k}\mathbf{x}_i^{Pb} - {}^{k}\mathbf{x}_i\right) + c_2\,{}^{(k+1)}\mathbf{r}_{i2}\times\left({}^{k}\mathbf{x}^{Gb} - {}^{k}\mathbf{x}_i\right) \tag{23} $$

$$ {}^{(k+1)}\mathbf{x}_i = {}^{k}\mathbf{x}_i + \tau\,{}^{(k+1)}\mathbf{v}_i \quad (\tau = 1) \tag{24} $$

in which w is the inertia weight whereas c_1 and c_2 are the so-called acceleration factors (they are called cognitive and social parameter, respectively). In Eq. (23), ${}^{(k+1)}\mathbf{r}_{1i}$ and ${}^{(k+1)}\mathbf{r}_{2i}$ are vectors whose n terms are random numbers uniformly distributed between zero and one, the symbol × denotes the term-by-term multiplication. The superscripts on the left and the subscripts on the right denote that a different couple of random vectors is needed for each particle at any iteration. The symbol ${}^{k}\mathbf{x}_i^{Pb}$ denotes the best previous position of the ith particle (also known as *pbest*):

$$ {}^{k}\mathbf{x}_i^{Pb} = \begin{cases} {}^{(k-1)}\mathbf{x}_i^{Pb} & \text{if } f\left({}^{k}\mathbf{x}_i\right) > f\left({}^{(k-1)}\mathbf{x}_i^{Pb}\right) \\ {}^{k}\mathbf{x}_i & \text{otherwise} \end{cases} \tag{25} $$

given that ${}^{0}\mathbf{x}_i^{Pb}={}^{0}\mathbf{x}_i$. According to the adopted definition for ${}^{k}\mathbf{x}^{Gb}$, there are two versions of PSOAs. If ${}^{k}\mathbf{x}^{Gb}$ is the best position among all the particles in the swarm (also known as *gbest*) such a version is called global PSOA (and the swarm is said to be fully informed or fully connected). On the other hand, if ${}^{k}\mathbf{x}^{Gb}$ is evaluated on a smaller number of adjacent particles (also known as *lbest*, ${}^{k}\mathbf{x}^{Lb}$) we have a local PSOA. In this paper, we will consider that all particles share information with each other about the best performer of the swarm, so that

$$ {}^{k}\mathbf{x}^{Gb} = \arg\min_{i=1,\ldots,N}\left\{ f\left({}^{k}\mathbf{x}_i^{Pb}\right)\right\} \tag{26} $$

The check on the maximum admissible velocity for each particle *i* is performed at iteration *k* in the following manner:

$$ {}^{k}v_{ij} = \begin{cases} \mathrm{sgn}\left[{}^{k}v_{ij}\right] v_j^{\max} & if \quad \left|{}^{k}v_{ij}\right| > \left|v_j^{\max}\right| \\ {}^{k}v_{ij} & otherwise \end{cases} \quad \forall j = 1,\ldots n \tag{27} $$

Another check is needed to verify that the particle is within the feasible search space:

$$ \left({}^{k}x_{ij}, {}^{k}v_{ij}\right) = \begin{cases} \left({}^{k}x_{ij}, {}^{k}v_{ij}\right) & if \;\; x_j^l \le {}^{k}x_j \le x_j^u \\ \left({}^{k}x_{ij} = x_j^l, {}^{k}v_{ij} = 0\right) & if \quad {}^{k}x_j < x_j^l \quad \forall j = 1,\ldots n \\ \left({}^{k}x_{ij} = x_j^u, {}^{k}v_{ij} = 0\right) & otherwise \end{cases} \tag{28} $$

In Eq. (28), the unfeasible particle's velocity is fixed to zero for the next iteration to avoid considering any points outside the search space.

A typical operator (called "craziness operator") is performed to increase the direction diversity in the swarm. Specifically, the adopted version for the craziness operator works on the particle's velocity only. Assigned a probability of craziness P_{cr}, the particle's velocity in Eq. (27) is replaced as follows:

$$ if \;\; r \le P_{cr} \rightarrow {}^{(k+1)}v_{ij} \sim U\left(-v_j^{\max}, v_j^{\max}\right) \;\; \forall j = 1,\ldots n \tag{29} $$

in which r is a uniform random number between 0 and 1, $U(\cdot)$ is the uniform probability density function. Once the particle's velocity is assigned by means of Eq. (29), a new position ${}^{(k+1)}\mathbf{x}_i$ is calculated for the particle by including this result in Eq. (24). A high value for P_{cr} results in (ineffective) pure random search, therefore its value should be less than 0.1 (0.05 in this study). Following iteratively this simple set of instructions, the swarm is expected to "fly" toward the global optimum of the problem. In our studies, the routine is stopped once a maximum number of iterations L is achieved.

4.2 Inertia weight and acceleration factors

The constriction factor χ is alternative to the use of the static inertia weight, initially proposed by [10] to replace the $\mathbf{v}^{\max}$ clamping. The constriction model describes the way of choosing w, c_1 and c_2 as follows:

$$ \begin{aligned} {}^{(k+1)}\mathbf{v}_i &= \chi\left[{}^{k}\mathbf{v}_i + c_1 {}^{(k+1)}\mathbf{r}_{i1} \times \left({}^{k}\mathbf{x}_i^{Pb} - {}^{k}\mathbf{x}_i\right) + c_2 {}^{(k+1)}\mathbf{r}_{i2} \times \left({}^{k}\mathbf{x}^{Gb} - {}^{k}\mathbf{x}_i\right)\right] \\ \chi &= \frac{2}{\left|2 - \varphi - \sqrt{\varphi^2 - 4\varphi}\right|} \\ \varphi &= c_1 + c_2 \ge 4 \end{aligned} \tag{30} $$

The new particle's position is computed as indicated in Eq. (24). Very typical values for this model are c_1=c_2=2.05, that is χ=0.73.

The model given by Eq. (23) can be modified by assuming both inertia weight and acceleration factors as dynamic parameters, that is: w=${}^{k}w$, c_1=${}^{k}c_1$, c_2=${}^{k}c_2$. In [11] is proposed a linearly decreasing inertia weight:

$$ {}^{k}w = \left({}^{0}w - {}^{L}w\right)\frac{L-k}{L} + {}^{L}w \tag{31} $$

where ${}^{0}w$ and ${}^{L}w$ are the initial and final values of the inertia weight (typically 0.9 and 0.4 respectively). Similarly, in [12] are proposed linearly iteration-dependent models for the acceleration factors:

$$\begin{aligned} {}^{k}c_1 &= \left({}^{0}c_1 - {}^{L}c_1\right)\frac{L-k}{L} + {}^{L}c_1 \\ {}^{k}c_2 &= \left({}^{0}c_2 - {}^{L}c_2\right)\frac{L-k}{L} + {}^{L}c_2 \end{aligned} \tag{32}$$

In several papers, ${}^{k}c_1$ changes from 2.5 to 0.5 and ${}^{k}c_2$ from 0.5 to 2.5.

4.3 Chaotic particle swarm optimization

One of the major drawbacks of the PSOA is its premature convergence, especially for search spaces with several local optima. In order to overcome this problem, some researchers proposed to introduce chaotic maps with certainty, ergodicity and pseudo-randomness property into PSOA so as to improve the global convergence [13]. Moreover, in [8] and [14] is stated that – due to the non-repetition of chaos – chaos-based optimization algorithms can carry out overall searches at higher speeds than stochastic ergodic searches that depend on probabilities. The ways in which the chaos entries into PSOAs are different but in this study we consider the most diffused one: in detail, we assume that chaotic maps are adopted to select the numerical values for the parameters of the particle's velocity in Eq. (23). Different numerical studies have been conducted for choosing the better chaotic maps. Looking for a synthesis of the documented results, we assume that the inertia weight is updated by adopting the logistic map [13]:

$${}^{(k+1)}\tilde{w} = \lambda\, {}^{k}\tilde{w}\left(1 - {}^{k}\tilde{w}\right) \quad with \ {}^{k}\tilde{w} \in (0,1) \tag{33}$$

where λ is assumed equal to 4 to obtain ergodicity in (0,1). The upper symbol ~ indicates that the corresponding quantity is evaluated by means of an opportune chaotic map. In our applications, the adopted value of the chaotic inertia weight are scaled within the interval [0.40,0.90]. About the acceleration factors, in [14] is proposed the use of the Zaslavskii map:

$${}^{(k+1)}\zeta_1 = \mathrm{mod}\left[{}^{k}\zeta_1 + \nu + \delta\, {}^{(k+1)}\zeta_2, 1\right] \tag{34}$$

$${}^{(k+1)}\zeta_2 = \cos\left(2\pi\, {}^{k}\zeta_1\right) + e^{-\rho}\, {}^{k}\zeta_2 \tag{35}$$

in which mod[·] is the modulus (signed remainder after division). The use of Zaslavskii map has been theoretically justified in [14] for virtue of its ergodicity and unpredictability, since a strange attractor with large Lyapunov exponent can be found for ν=400, ρ=3 and δ=12.6695 (in this case, ${}^{k}\zeta_2 \in$ [-1.0512,1.0512]). Therefore, in [14] is stated that a Zaslavskii map-based chaotic PSOA should be more capable of escaping from local optima than random search. In our applications, both chaotic acceleration factors are functions based on the results of Eq. (35), but final values are scaled within the interval [0.50,2.50].

4.4 Passive congregation

The dynamic of natural swarms can be modeled by taking into account two grouping forms [15]:

- Aggregation, that is a grouping by environmental forces. Two types of aggregation forms can be identified. The passive aggregation is a passive grouping due to physical phenom-

ena (i.e., transport caused by water currents) whereas the active aggregation is a grouping by attractive resources (i.e., food or space within the environment);

- Congregation, that is a grouping by social forces (it depends on the group itself and not on the environment). Also in this case two different forms of congregation can be analyzed. The passive congregation is the attraction between members of the group without the existence of observable social behaviors and therefore it looks as a random phenomenon. On the other hand, the social congregation happens under active information transfer, so that the behavior of the group depends on the relations among the members of the group.

It has been pointed out in [15] that the third addend of the standard PSOA in Eq. (23) models an active aggregation rather than a passive congregation because ${}^{k}\mathbf{x}_{Gb}$ can be regarded (using a biologic metaphor) as "the place with most food". Therefore, the standard model in Eq. (23) does not incorporate a congregation form. Starting from this consideration, in [15] is proposed a new rule for updating the particle's velocity: by including a passive congregation term the information sharing within the swarm may be improved and the recognition of the search space as well. Accounting for the passive congregation, the particle's velocity is updated as follows [15]:

$$ {}^{(k+1)}\mathbf{v}_i = w\,{}^{k}\mathbf{v}_i + c_1\,{}^{(k+1)}\mathbf{r}_{i1}\times\left({}^{k}\mathbf{x}_i^{Pb} - {}^{k}\mathbf{x}_i\right) + c_2\,{}^{(k+1)}\mathbf{r}_{i2}\times\left({}^{k}\mathbf{x}^{Gb} - {}^{k}\mathbf{x}_i\right) + c_3\,{}^{(k+1)}\mathbf{r}_{i3}\times\left({}^{k}\mathbf{x}_{rand} - {}^{k}\mathbf{x}_i\right) \quad (36) $$

in which ${}^{k}\mathbf{x}_{rand}$ is a particle selected randomly from the swarm, ${}^{(k+1)}\mathbf{r}_{3i}$ is a vector whose terms are random numbers uniformly distributed between zero and one and c_3 is another acceleration factor (called passive congregation coefficient, a constant positive real value). The adopted (constant) numerical values for the control parameters in Eq. (36) are taken from [15].

5 IDENTIFICATION VIA GENETIC ALGORITHM

Genetic algorithms are well known non-classical techniques for parametric identification: during a succession of generations, these methods generate new points in the admissible search space by applying operators on the current solutions set and "statistically" moving toward more optimal places in virtue of the Darwinian strife for survival. A detailed state-of-the-art review about genetic algorithm based mechanical system identification can be found in [16].

A modified real-coded genetic algorithm [17] for parametric identification of mechanical system is considered in this paper. The algorithm – whose acronym is MGAR – utilizes several subpopulations and a migration operator with a ring topology is periodically performed to allow the interaction between them. For each subpopulation, a specialized medley of recent genetic operators (crossover and mutation) has been adopted and is briefly discussed. The final algorithm includes an operator based on the auto-adaptive asexual reproduction of the best individual in the current subpopulation. This latter was introduced to avoid a long stagnation at the start of the evolutionary process due to insufficient exploration as well as to attempt an improved local exploration around the current best solution at the end of the search. The original algorithm included a search space reduction technique, but it is not considered in this paper because of the small number of unknown parameters to be identified. This algorithm was successfully adopted for nonlinear [17] and large linear system identification [18]. The interested reader can refer to [17] and [18] for more information about it and the adopted numerical values for the embedded control parameters.

6 NUMERICAL RESULTS

A large numerical investigation is conducted to assess the performances of the above presented non-classical identification techniques for parametric identification of a nonlinear viscous damper subject to various dynamic loads (harmonic and earthquake loading). The effect of the noise contamination in the reference response is also studied.

6.1 Problem data and non-classical identification methods under investigation

A list of the considered non-classical identification methods is given in Tab. 1.

Algorithm	Short description
DEA01	A DEA whose mutation operator is given by Eq. (9) and with binomial crossover as in Eq. (14)
DEA02	A DEA whose mutation operator is given by Eq. (10) and with binomial crossover as in Eq. (14)
DEA03	A DEA whose mutation operator is given by Eq. (11) and with binomial crossover as in Eq. (14)
DEA04	A DEA whose mutation operator is given by Eq. (12) and with binomial crossover as in Eq. (14)
DEA05	A DEA whose mutation operator is given by Eq. (13) and with binomial crossover as in Eq. (14)
DEA06	A DEA with adaptive mutation – as in Eq. (16) and Eq. (17) – and a free-parameter crossover given by Eq. (22), see [7]
PSOA01	A PSOA whose velocity model is Eq. (23), with inertia weight as in Eq. (31), social and cognitive factors as in Eq. (32)
PSOA02	A PSOA in which the velocity updating rule (based on the use of the constriction factor) is given by Eq. (30)
PSOA03	A PSOA based on the use of chaotic maps (so-called chaotic PSOA) for both inertia weight and acceleration factors
PSOA04	A PSOA with passive congregation in which the velocity updating rule is given by Eq. (36)
MGAR	A modified multi-species real-coded genetic algorithm with specialized operators for each subpopulation, see [17] and [18]

Table 1: List of non-classical identification methods under investigation.

The parametric identification of the viscous damper is performed by solving the optimization problem in Eq. (7) whose cost function is given in Eq. (8). For this numerical investigation, the adopted mechanical model is that in Eq. (6) and the numerical values of the involved parameters are taken from [5]: M=1000, C_1=100, C_α=400, K_1=1000 and α=0.20. The set of parameters to be identified is $\mathbf{x}=\{M, C_1, K_1, C_\alpha, \alpha\}$ and $\mathbf{x}^*$ is its true real value. Lower and upper bounds are, $\mathbf{x}^l=0.10\mathbf{x}^*$ and $\mathbf{x}^u=2.00\mathbf{x}^*$, respectively. The population size and the maximum number of iterations are N=50 and L=400, respectively.

6.2 Nonlinear viscous damper subject to harmonic base motion

The viscous damper is subject to harmonic base motion:

$$p(t) = -Ma_g^{\max} \sin(\Omega t) \tag{37}$$

in which a_g^{max}=0.25g (g is the gravity acceleration) and Ω is given in Tab. 2 as function of the natural frequency of the system, that is $\omega = \sqrt{(K_1/M)}$.

Initial velocity and initial displacement are both equal to zero. The total number of samples is S = 2000. Unit of measures are arbitrary but consistent.

Load case	Ω/ω
L1	1.00
L2	0.50
L3	2.00

Table 2: Load cases.

Mean results over thirty distinct runs (that is, with different initial populations) are presented in Fig. 1 (for M), Fig. 2 (for C_1), Fig. 3 (for K_1), Fig. 4 (for C_α) and Fig. 5 (for α). The black horizontal solid line denotes the true parameter value.

A general overview of the obtained results leads to the following considerations:

- Non-classical identification methods provide an effective way for the parametric identification of nonlinear viscous dampers subject to harmonic-type dynamic loading, because the final errors are acceptable for practical applications.
- The load case L1 causes the most critical situation for the parametric identification of nonlinear viscous dampers. This is may be imputable to the use of harmonic excitation whose frequency coincides with that of the viscous damper.
- The DEA06 and MGAR are the best competitor for this numerical application because the identified parametric values are very close to the exact solution. Their performance in the parametric identification are strongly better than the others for the load case L1.

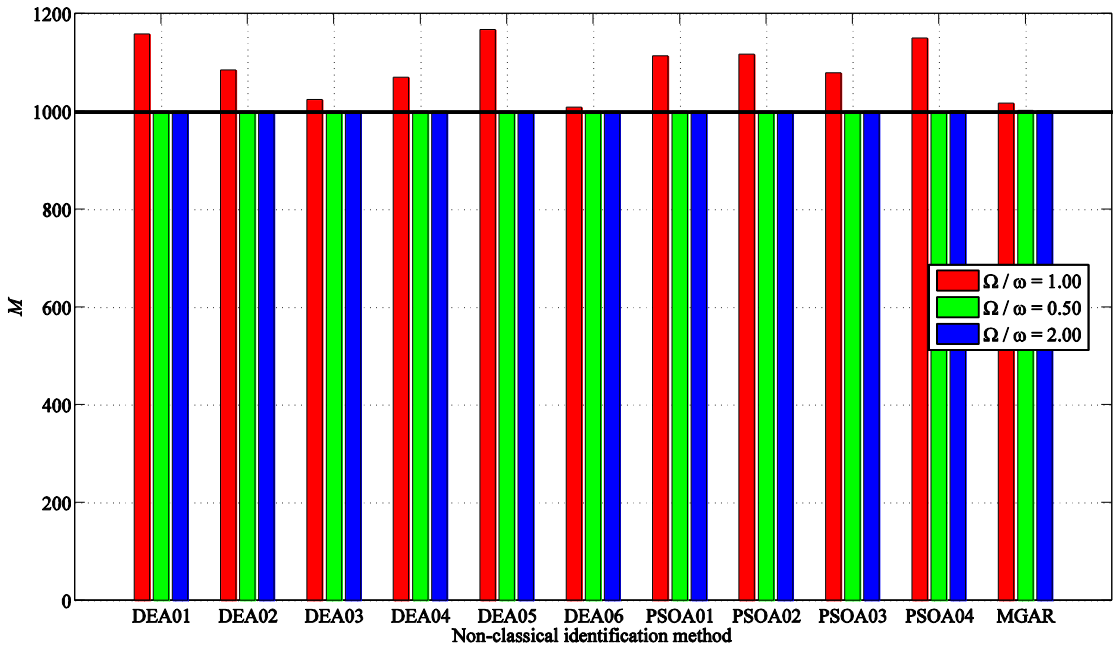

Figure 1: Identification results for M.

However, it was observed that all non-classical methods can achieve the exact solution of the identification problem by increasing the number of objective function evaluations. In this perspective, DEA06 and MGAR are more competitive than the others from a computational standpoint.

A more detailed inspection of the plotted results may provide further practical information. For instance, it appears that DEAs and PSOAs lead to comparable final results. There are no significant differences within the standard DEAs. On the other hand, the chaotic PSOA (labeled as PSOA03 in Tab. 01) is slightly better than the others.

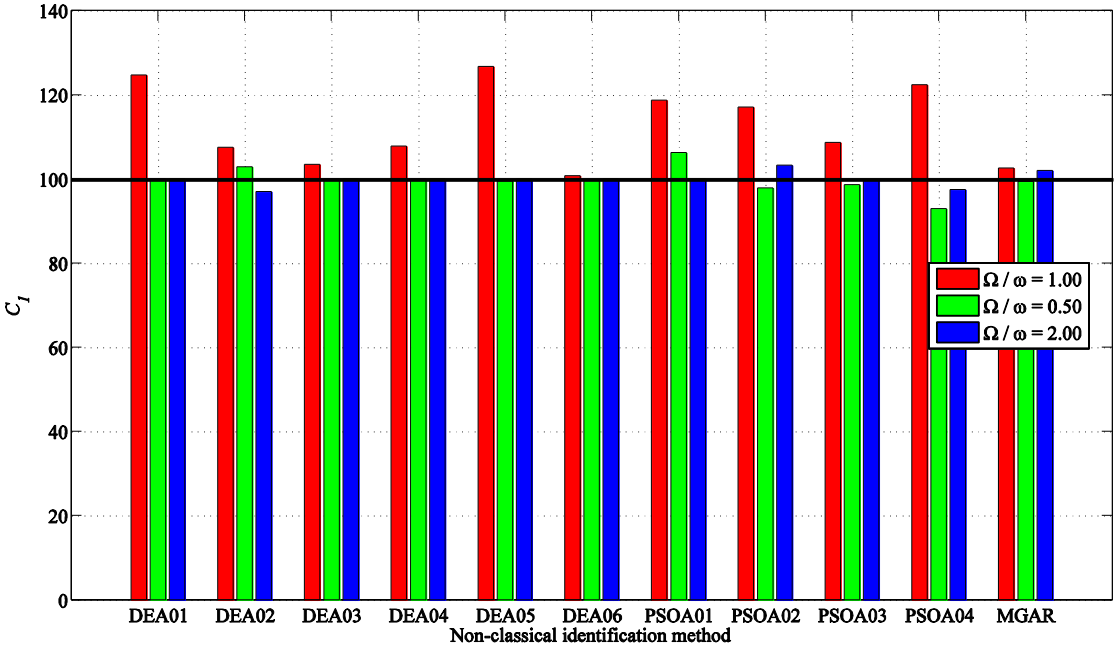

Figure 2: Identification results for C_1.

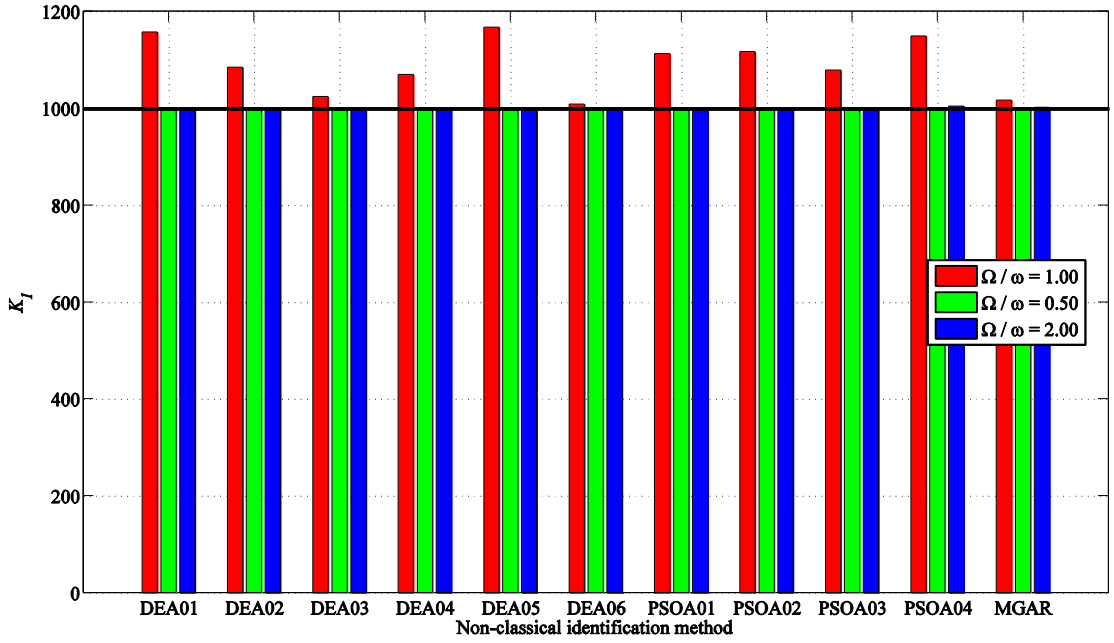

Figure 3: Identification results for K_1.

The most critical parameters to be identified is C_α: as it can be seen in Fig. 4, its numerical value for the load case L1 is approximately identified by the most of the investigated techniques (not so good results are obtained by using DEA01, DEA05, PSOA01, PSOA02 and PSOA04). For the most critical loading condition (L1), it is observed that (*i*) the identified values of M, C_1 and K_1 (mean values over thirty runs) are greater than the exact ones whereas (*ii*) the identified values of C_α (mean values over thirty runs) are lower than the exact ones.

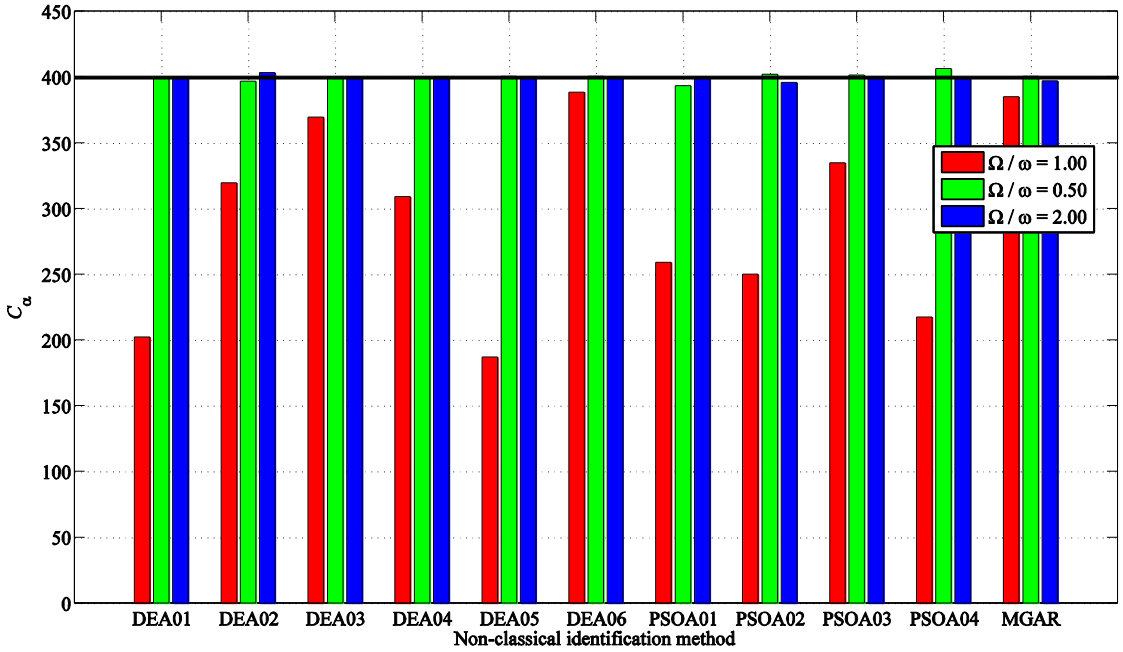

Figure 4: Identification results for C_α.

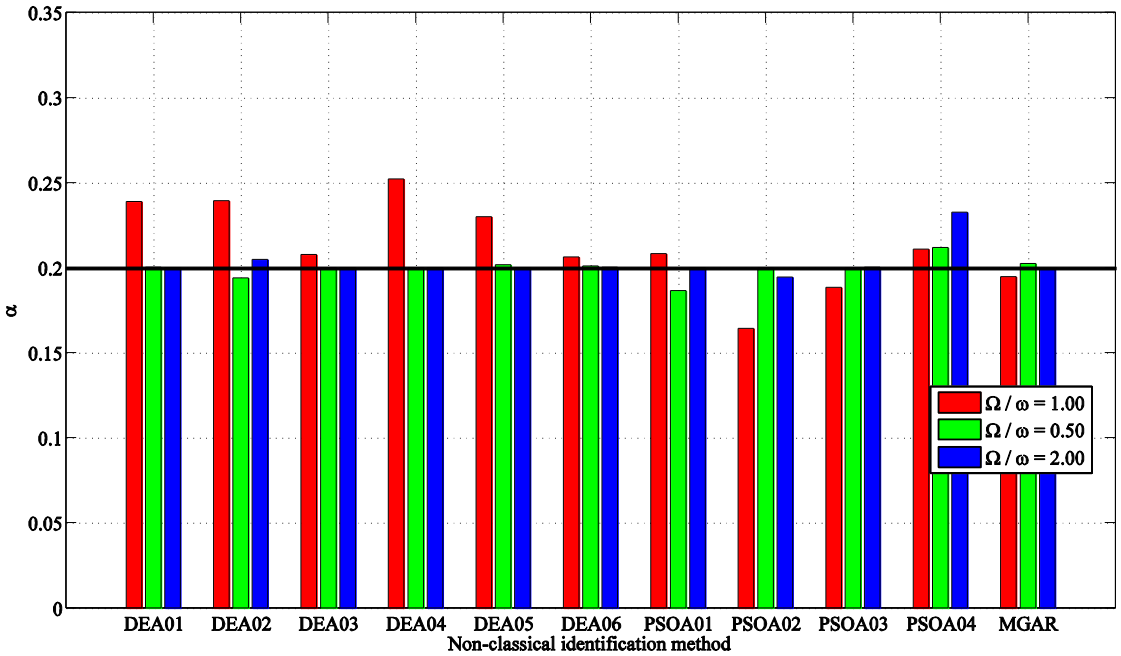

Figure 5: Identification results for α.

Some samples of the convergence histories for DEA06 are shown in Fig. 6 (for load case L1), Fig. 7 (for load case L2) and Fig. 8 (for load case L3). As above, the black horizontal solid line denotes the true parameter value. The objective function shows a small number of stagnations (number of iterations without improvements). This means that the exploration phase of the evolutionary search for DEA06 is very efficient.

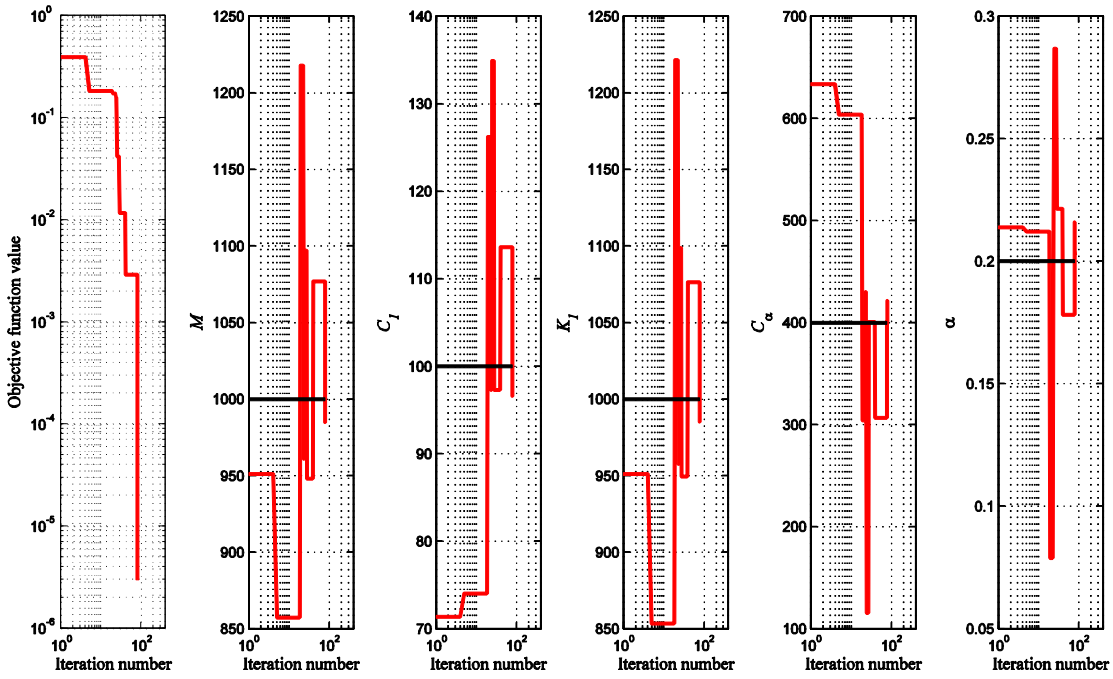

Figure 6: A sample of the convergence histories for DEA06 (load case L1).

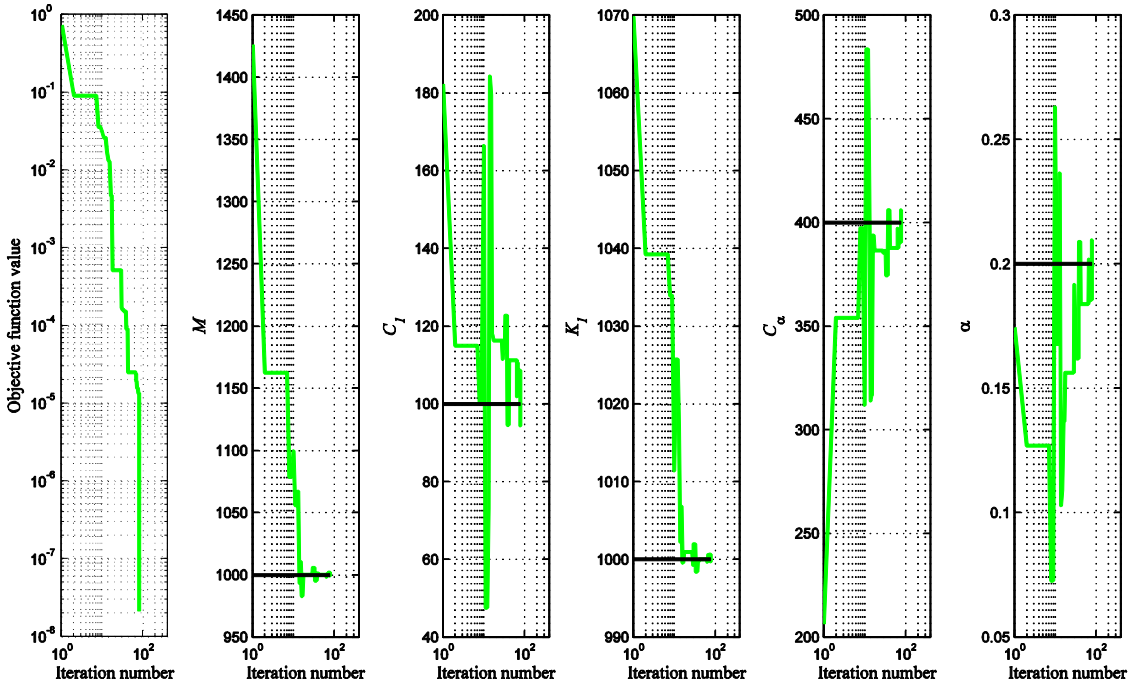

Figure 7: A sample of the convergence histories for DEA06 (load case L2).

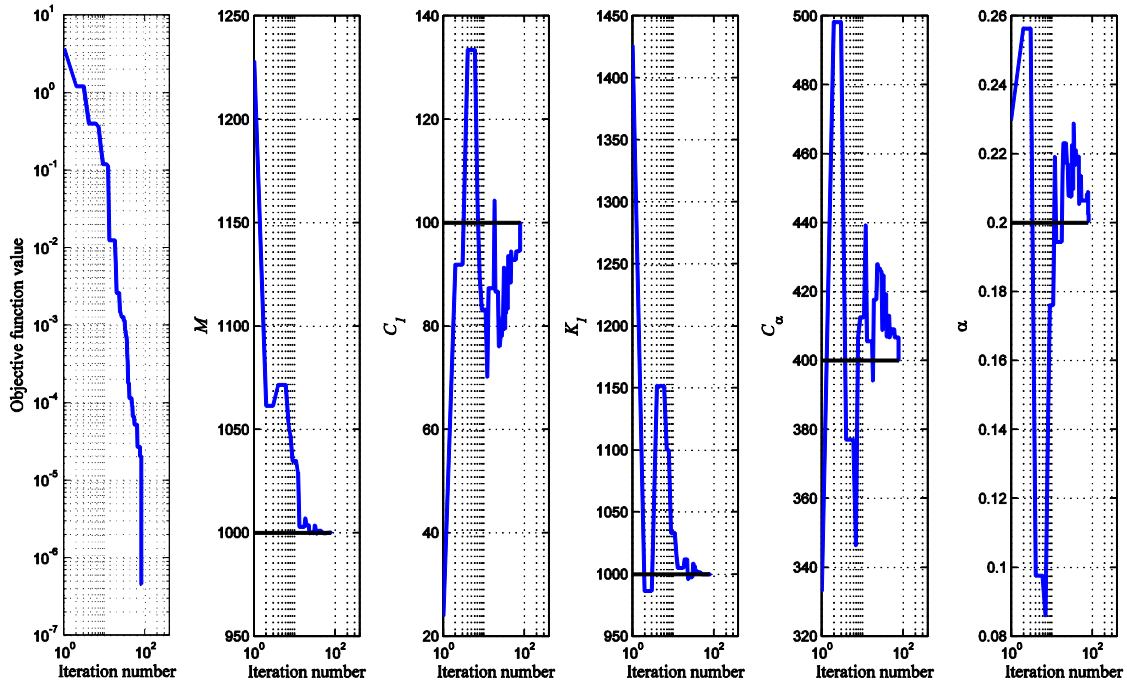

Figure 8: A sample of the convergence histories for DEA06 (load case L3).

Convergence histories of the model parameters confirm the effectiveness of DEA06 in parametric identification of the nonlinear viscous damper because a quasi exact results is achieved once 200÷300 iterations are completed. As a consequence, the total elaboration time can be reduced without jeopardizing the correctness of the identification process.

6.3 Nonlinear viscous damper subject to earthquake motion

The same nonlinear viscous dampers was identified under, both, white random noise and earthquake excitation. Using the non-classical methods under investigation (as they are listed in Tab. 1), all the model parameters were exactly identified (i.e., to four decimal digits). It has been observed that the final accuracy is slightly better than the obtained one for harmonic loading. It is an expected results, because the efficiency of the identification depends on the information contained in the input-output data: in this sense, harmonic loads with a low frequencies content are a limited excitation source. Herein, only results for a viscous damper subject to a real earthquake record are shown. Thus, the dynamic load is:

$$p(t) = -Ma_g(t) \tag{38}$$

in which a_g is the adopted earthquake record (for this numerical application, the El Centro earthquake is considered). Moreover, in order to study the detrimental effect of the noise contamination, a noisy reference system response is taken into account. A uniform-type noise was considered whit a noise-to-signal-ration (NSR) equal to 15%. The obtained noisy signal has not been subject to de-noising.

The results – summarized in Fig. 9 – demonstrate that DEA06 is relatively insensitive to moderate noise levels. The noise robustness of non-classical identification methods is well known in the current literature and it depends on the implicit parallelism in such numerical techniques [7][17]. Comparing the identification results by using a noise-free (solid lines in Fig. 9) and a noisy reference response, it is observed that:

- Because of the noise contamination, the minimum value of the objective function in Eq. (8) is not equal to zero. The final minimum value of the objective function under noisy signals may be very far from the ideal one (that is, equal to zero).
- The role of the exploration phase increases as the NSR value grows. In fact, the convergence histories toward the optimal solutions using noise-free data are faster than those for a NSR=15%. It is observed that the initial parts of the evolutionary search are more irregular when using a noisy system response, thus highlighting the importance of the exploration stage.

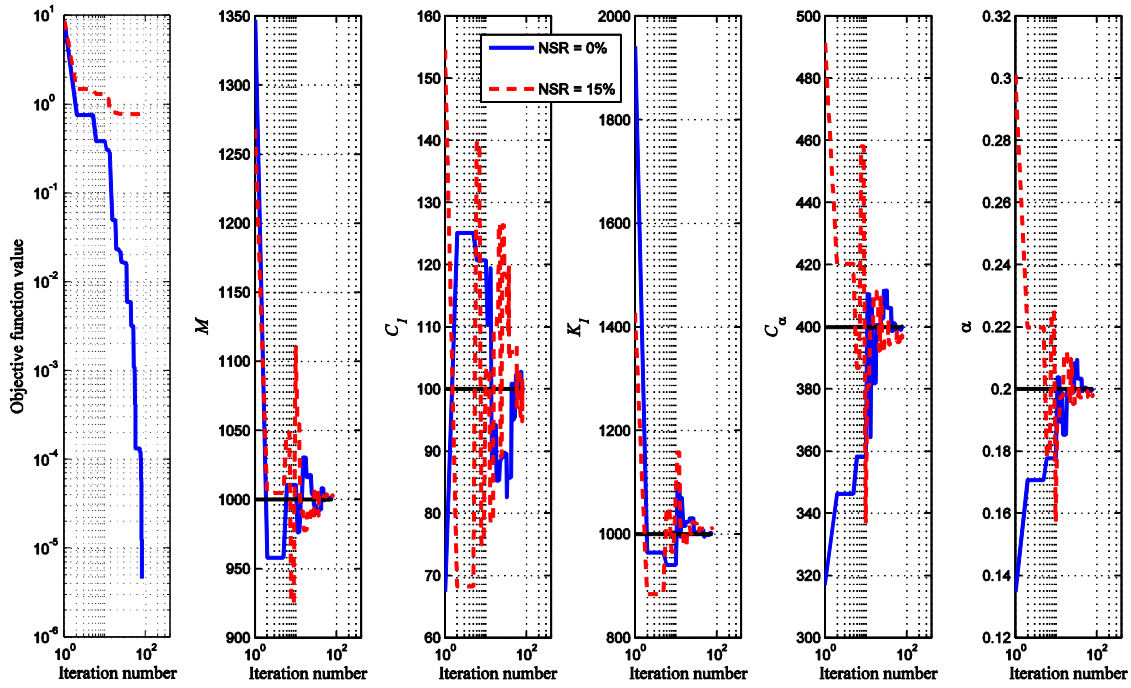

Figure 9: Convergence histories for DEA06 using free-noise and noisy reference response.

7 EXPERIMENTAL RESULTS

The synthesis of the conducted numerical studies provide positive evidences about the reliability of the investigated non-classical identification techniques for parametric identification of nonlinear viscous dampers. Moreover, useful aspects regarding the computational efficiency and the robustness against the instrumental noise were addressed. Nonetheless, the real viscous damper response may be more complicated and neglected nonlinearities can be relevant. Therefore it is essential to assess the applicability of these methods by using experimental data. To this end, some experimental tests were performed on a full-scale nonlinear viscous damper.

7.1 Experimental tests

?? [19]

7.2 Results of the identification based on experimental data

??

8 CONCLUSIONS

??

9 ACKNOLEDGMENTS

??

REFERENCES

[1] T.T. Soong, B.F. Spencer Jr, Supplemental energy dissipation: state-of-the-art and state-of-the practice. *Engineering Structures*, **24**, 243-259, 2002.

[2] H.B. Yun, F. Tasbighoo, S.F. Masri, J.P. Caffrey, R.W. Wolfe, N. Makris, C. Black, Comparison of Modeling Approaches for Full-scale Nonlinear Viscous Dampers. *Journal of Vibration and Control*, **14**, 51-76, 2008.

[3] C.G. Koh, Y.F. Chen, C.Y. Liaw, A hybrid computational strategy for identification of structural parameters. *Computers and Structures*, **81**, 107-117, 2003.

[4] G. Terenzi, Dynamics of SDOF Systems with Nonlinear Viscous Damping. *Journal of Engineering Mechanics*, 125, 956-963, 1999.

[5] A. Della Valle, Sulla progettazione in zona sismica di strutture dotate di dissipatori fluido-viscosi. Ph. D. Thesis, 2008 (in Italian).

[6] R. Storn, K. Price, Differential evolution – A simple and efficient heuristic for global optimization over continuous space. *Journal of Global Optimization*, **4**, 359-431, 1997.

[7] G. Quaranta, G. Monti, G.C. Marano, Parameters identification of Van der Pol-Duffing oscillators via particle swarm optimization and differential evolution. *Mechanical Systems and Signal Processing*, **24**, 2076-2095, 2010.

[8] L.S. Coelho, A quantum particle swarm optimizer with chaotic mutation operator. *Chaos, Solitons and Fractals*, **37**, 1409-1418, 2008.

[9] Y. Shi, R. Eberhart, A modified particle swarm optimizer. *IEEE World Congress on Computational Intelligence*, Anchorage, AK, USA, May 4-9, 1998.

[10] M. Clerc, The swarm and the queen: towards a deterministic and adaptive particle swarm optimization. *Proceedings of the congress on evolutionary computation (CEC 1999)*, Washington DC, USA, July 6-9, 1999.

[11] Y. Shi, R. Eberhart, Empirical study of particle swarm optimization, *Congress on evolutionary computation (CEC 1999)*, Washington DC, USA, July 6-9, 1999.

[12] A. Ratnaweera, S.K. Halgamuge, H.C. Watson, Self-Organizing Hierarchical Particle Swarm Optimizer With Time-Varying Acceleration Coefficients. *IEEE Transactions on Evolutionary Computation*, **8**, 240-255, 2004.

[13] J. Chuanwen, E. Bompard, A hybrid method of chaotic particle swarm optimization and linear interior for reactive power optimisation. *Mathematics and Computers in Simulation*, **68**, 57-65, 2005.

[14] L.S. Coelho, B.M. Herrera, Fuzzy Identification Based on a Chaotic Particle Swarm Optimization Approach Applied to a Nonlinear Yo-yo Motion System. *IEEE Transactions on Industrial Electronics*, **54**, 3234-3245, 2007.

[15] S. He, Q.H. Wu, J.Y. Wen, J.R. Saunders, R.C. Paton, A particle swarm optimizer with passive congregation. *Biosystems*, **78**, 135-47, 2004.

[16] G.C. Marano, G. Quaranta, G. Monti, Genetic Algorithms in Mechanical Systems Identification: State-of-the-art Review, in *Soft Computing in Civil and Structural Engineering* (Chapter 2), B.H.V. Topping and Y. Tsompanakis, Eds., Stirlingshire (Scotland): Saxe-Coburg Publications, 2009.

[17] G. Monti, G. Quaranta, G.C. Marano, Genetic-algorithm-based strategies for dynamic identification of nonlinear systems with noise corrupted response, *Journal of Computing in Civil Engineering*, **24**, 173-187, 2010.

[18] G.C. Marano, G. Quaranta, G. Monti, Modified Genetic Algorithm for the Dynamic Identification of Structural Systems Using Incomplete Measurements. *Computer Aided Civil and Infrastructure Engineering*, article in press, 2010.

[19] Norme Tecniche per le Costruzioni, D.M. 14 gennaio 2008, G.U. n. 29, 4 febbraio, n. 30, 2008.